

# Fruit of *Hovenia dulcis* Thunb. Induces Nonshivering Thermogenesis through Mitochondrial Biogenesis and Activation by SIRT1 in High-Fat Diet-Fed Obese Mice and Primary Cultured Brown Adipocytes

Gahee Song, Hye-Lin Kim, Yunu Jung, Jinbong Park, Jun Hee Lee, Kwang Seok Ahn, Hyun Jeong Kwak, and Jae-Young Um\*

 Cite This: *J. Agric. Food Chem.* 2020, 68, 6715–6725

 Read Online

ACCESS |

 Metrics & More

 Article Recommendations

 Supporting Information

**ABSTRACT:** Brown adipocytes, which contain abundant mitochondria, use stored energy as fuel during a process named nonshivering thermogenesis. Thus, the pharmacological activation of thermogenesis in brown adipose tissue (BAT) has become a promising target for treating obesity. We investigated the effect of fruit of *Hovenia dulcis* Thunb. (FHD), a frequently used herbal treatment for liver diseases, on thermogenesis and its mechanism using primary cultured brown adipocytes and BAT of high-fat-diet (HFD)-induced obese mice. Thermogenesis-related factors including UCP1 and PGC1 $\alpha$  increased with FHD treatment. FHD also increased mitochondrial biogenesis and activation factors such as nuclear respiratory factor (NRF)1 and oxidative phosphorylation (OXPHOS) complex. Furthermore, FHD increased the intercellular nicotinamide adenine dinucleotide (NAD<sup>+</sup>) level and sirtuin 1 (SIRT1) activity, which may be responsible for the activation of the thermogenic reaction. Overall, our results suggest that FHD can be a novel option for obesity treatment due to its thermogenic action through mitochondrial biogenesis and activation.

**KEYWORDS:** obesity, BAT, thermogenesis, mitochondria, SIRT1, *Hovenia dulcis* Thunb.

## INTRODUCTION

Brown adipose tissue (BAT) regained interest after its identification in adult humans using fluorodeoxyglucose positron emission tomography (PET) in 2009.<sup>1</sup> Through intensive research, it has been demonstrated that the tissue can be activated in response to multiple stimuli, such as cold exposure, insulin, and  $\beta$ 3-adrenergic receptor agonist.<sup>2–4</sup> These observations inspired researchers to study BAT as a potential new target for obesity treatment.

Adipose tissue is subcategorized into white and brown adipose tissues. White adipose tissue (WAT) is a storage place, playing a role in accumulating lipid. Excessive lipid accumulation is known to be a major cause of coronary cardiovascular diseases, obesity, hyperlipidemia, and hypertension.<sup>5,6</sup> In contrast, BAT possesses abundant mitochondria with numerous multilocular lipid droplets and plays a crucial role in using stored lipid by dissipating heat: nonshivering thermogenesis.<sup>7</sup> Thus, BAT can regulate body weight, lipid metabolism, and body temperature: the whole-body energy metabolism.<sup>8</sup> BAT is found only in mammals and humans; it is at its highest levels at the time of birth and decreases with age.<sup>9</sup> The amount of BAT in adults is highly correlated with the degree of body mass index, implying that BAT may play a significant role in preventing and treating obesity.<sup>10</sup> Therefore, BAT stimulation via mitochondrial activation can be a key target to improve obesity.

The mitochondria of BAT are equipped with a special protein called uncoupling protein 1 (UCP1), which short-circuits the electron transport chain to shift the normal adenosine 5'-triphosphate (ATP)-producing action of mito-

chondrial membrane potential toward heat production.<sup>11</sup> Through this, BAT can increase energy expenditure and metabolism without any physical activity, due to its abundant mitochondria.<sup>12</sup> Metabolic processes of mitochondria in adipose tissue are largely dependent on nicotinamide adenine dinucleotide (NAD<sup>+</sup>) homeostasis; thus, disrupted NAD<sup>+</sup> homeostasis, which leads to mitochondrial dysfunction, is one of the major causes of obesity and other metabolic disorders.<sup>13</sup> Mitochondrial metabolism is regulated by NAD-dependent enzymes such as sirtuins (SIRTs) and poly-(adenosine 5'-diphosphate (ADP)-ribose) polymerases.<sup>14,15</sup> Among them, SIRT1 is an ortholog of the nuclear NAD<sup>+</sup>-dependent protein deacetylase. SIRT1 activity is regulated by the cellular environment closely associated with NAD<sup>+</sup> availability. For example, a high-energy status such as inflammatory responses downregulates cellular NAD<sup>+</sup> levels, and this change in the NAD<sup>+</sup> level reduces SIRT1 activity.<sup>16</sup> Therefore, SIRT1 is considered an important regulator of various cellular metabolic processes from energy metabolism and stress response.<sup>17</sup>

*Hovenia dulcis* Thunb., a member of the Rhamnaceae family, is a native tree in Asian countries including Korea, China, and Japan. Most of the parts of this tree, i.e., fruits, seeds, leaves,

**Received:** February 23, 2020

**Revised:** May 25, 2020

**Accepted:** May 25, 2020

**Published:** May 25, 2020

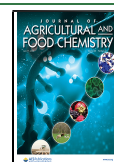


Table 1. Primer Sequences Used for qPCR<sup>a</sup>

genes	forward (5'–3')	reverse (5'–3')
<i>Ucp1</i>	AGGCTTCCAGTACCATTAGGT	CTGAGTGAGGCCAAAGCTGATTT
<i>Ppargc1a</i>	TTCATCTGAGTATGGAGTCGT	GGGGGTGAAACCACTTTTGTAA
<i>Sirt3</i>	ATCCCGGACTTCAGATCCCC	CAACATGAAAAGGGCTTGGG
<i>Prdm16</i>	CCAAGGCAAGGGCGAAGAA	AGTCTGGTGGGATTGGAATGT
<i>Cox4</i>	ATTGGCAAGAGAGCCATTTCTAC	CACGCCGATCAGCGTAAGT
<i>Cox8</i>	TGTGGGGATCTCAGCCATAGT	AGTGGGCTAAGACCCATCCTG
<i>Nrf1</i>	CCACGTTGGATGAGTACACG	CAGACTCGAGGTCTTCCAGG
<i>Cidea</i>	TGACATTCATGGGATTGCAGAC	GGCCAGTTGTGATGACTAAGAC
<i>Cyts</i>	CCAATCTCCACGGTCTGTTC	ATCAGGGTATCCTCTCCCCAG
<i>Dnm1l</i>	CAGGAATTGTTACGGTTCCTTAA	CCTGAATTAACCTGTCCCGTGA
<i>Mfn1</i>	ATGGCAGAAACGGTATCTCCA	CTCGGATGCTATTTCGATCAAGTT
<i>Gapdh</i>	AGGTCGGTGTGAACGGATTTG	TGTAGACCATGTAGTTGAGGTCA

<sup>a</sup>*Ucp1*, uncoupling protein 1; *Ppargc1a*, peroxisome proliferative activated receptor;  $\gamma$ , coactivator 1  $\alpha$ ; *Sirt3*, sirtuin 3; *Prdm16*, PR domain containing 16; *Cox4*, cytochrome *c* oxidase subunit 4I1; *Cox8*, cytochrome *c* oxidase subunit 8b; *Nrf1*, nuclear respiratory factor 1; *Cidea*, cell-death-inducing DNA fragmentation factor,  $\alpha$  subunit-like effector A; *Cyts*, cytochrome *c*; *Dnm1l*, dynamin 1-like; *Mfn1*, mitofusin-1; *Gapdh*, glyceraldehyde-3-phosphate dehydrogenase.

roots, and bark, are used in traditional Korean medicine for various purposes including inflammation and liver diseases. The fruits of *H. dulcis* Thunb. (FHD) contain an extensive variety of pharmaceutically active compounds, such as ampelopsin, taxifolin, myricetin, and quercetin.<sup>18</sup> Ji et al. reported its beneficial effects on diabetes, reducing blood sugar, and hepatic glycogen.<sup>19</sup> In our previous study, we investigated and reported the effect of FHD on the adipogenesis in 3T3-L1 adipocytes. In brief, FHD modulated adipogenic factors through activation of AMP-activated protein kinase (AMPK)- $\alpha$ , resulting in decreased lipid accumulation.<sup>20</sup> However, its thermogenic action and the underlying mechanism have not been verified to date. In this study, we studied whether FHD can affect the nonshivering thermogenesis pathway using BAT of high-fat-diet (HFD)-induced obese C57BL/6 mice and primary cultured brown adipocytes.

## MATERIALS AND METHODS

**Chemical Reagents.** Dulbecco's modified Eagle's medium (DMEM), fetal bovine serum (FBS), and antibiotics (penicillin–streptomycin–glutamine) were purchased from Gibco BRL (NY). Oil Red-O powder, insulin, 3-isobutylmethylxanthine (IBMX), and dexamethasone (DEX) were from Sigma Chemical Co. (St. Louis, MO). Olaparib (10621) and NAD<sup>+</sup> (16077) were purchased from Cayman Chemical Company (Ann Arbor, MI).

**Antibodies.** SIRT3 (5490S), UCP1 (14670S), nuclear respiratory factor (NRF)2 (12721S), NRF1 (12381S), AMPK $\alpha$  (2532S), pAMPK $\alpha$  (T172) (2535S), and Cytochrome C (CytC) (4272S) were from Cell Signaling Technology (Beverly, MA). Glyceraldehyde-3-phosphate dehydrogenase (GAPDH) (sc-32233), mitochondrial preprotein translocases of the outer membrane 20 (TOM20) (sc-17764), mitochondrial fission 1 (FIS1) (sc-376447), and mitofusin-1 (MFN1) (sc-166644) were from Santa Cruz Biotechnology (Paso Robles, CA). Peroxisome proliferator-activated receptor  $\gamma$  coactivator 1 $\alpha$  (PGC1 $\alpha$ ) (ab54481), PR domain containing 16 (PRDM16) (ab106410), and total oxidative phosphorylation (OXPHOS) (ab110413) were from Abcam (Cambridge, MA). UCP1 (U6382) was from GeneTex (Irvine, CA).

**Preparation of the FHD Extract.** The water extract of FHD was provided by SEROM Co., Ltd. (Jangheung, Korea).

**Ethical Statement.** All animal experiments were performed according to the Guide for the Care and Use of Laboratory Animals, approved by the Institutional Review Board of Kyung Hee University (confirmation number: KHUASP (SE)-13-012).

**Animal Experiments.** Male C57BL/6 mice (4 weeks old) were purchased from Daehan Biolink (Eumsung, Korea) and maintained

for 1 week. To induce obesity, mice were fed a 60% HFD (rodent diet D12492; Research Diet, New Brunswick, NJ) for 4 weeks before administering vehicle or FHD (5 mg/kg/day). Food and water were provided ad libitum. Mice were then randomly divided into two groups ( $n = 6$  per group): (1) HFD and (2) HFD supplemented with FHD extract at 5 mg/kg/day, the dose of which was decided based on a previous study.<sup>21</sup> An additional 7 week administration was carried out in the two groups. Mice fed a normal diet (ND) (CJ Feed Co., Ltd., Seoul, Korea) were used as the normal control group. Body weight and food intake were measured once a week. After a total of 11 weeks at the end of the experiment, mice were anesthetized under CO<sub>2</sub> asphyxiation, blood was collected via cardiac puncture, and tissues were dissected and stored at  $-80^{\circ}\text{C}$  until further use. Serum was separated immediately after blood collection. The composition of diets is displayed in Table S1.

**Blood Serum Analysis.** Serum glucose, total cholesterol (TC), low-density lipoprotein-cholesterol (LDL-C), high-density lipoprotein-cholesterol (HDL-C), alanine transaminase (ALT), aspartate aminotransferase (AST), and creatinine levels were analyzed using enzymatic colorimetric methods by Seoul Medical Science Institute (Seoul, Korea).

**Hematoxylin and Eosin (H&E) Staining.** Hematoxylin and eosin (H&E) staining was performed as previously described.<sup>22</sup> Photographs were taken under an EVOS M7000 system (Thermo Fisher Scientific, Waltham, MA).

**Immunofluorescence (IF) Assay.** Cells and tissues were fixed using 10% formalin and blocked with 5% bovine serum albumin (BSA) for 1 h. Then, they were incubated with the indicated primary antibodies for UCP1, PGC1 $\alpha$ , TOM20, MFN1, and FIS1 overnight at  $4^{\circ}\text{C}$  and followed by incubation with the Alexa Flour 488- or 633-conjugated secondary antibody (1:1000). The fluorescence signal was detected using an EVOS M7000 system (Thermo Fisher Scientific, Waltham, MA).

### Cell Isolation, Culture, and Adipocyte Differentiation.

Brown preadipocytes were isolated from newborn FVB mice (Daehan Biolink, Eumsung, Korea) based on the method of Klein et al.<sup>23</sup> Briefly, interscapular BAT was isolated, minced, and subjected to collagenase digestion. The digested tissue was filtered, and collected cells were centrifuged and resuspended in 10 mL of culture medium (DMEM containing 25 mM glucose, 20% FBS, 20 mM *N*-(2-hydroxyethyl)piperazine-*N'*-ethanesulfonic acid (Hepes)) in a 100 mm plate, grown at  $37^{\circ}\text{C}$  and 5% CO<sub>2</sub>. Primary brown preadipocytes were differentiated into mature brown adipocytes 48 h after full confluence (day 0) by a differentiation medium (DM) consisting of DMEM plus 10% FBS and supplemented with 0.5 mM IBMX, 0.5  $\mu\text{M}$  DEX, 20 nM insulin, 125 mM indomethacin, and 1 nM 3,3',5-triiodo-L-thyronine (T3). On day 4, the medium was replaced with a maintenance medium composed of DMEM, 10% FBS, 1 nM T3, and

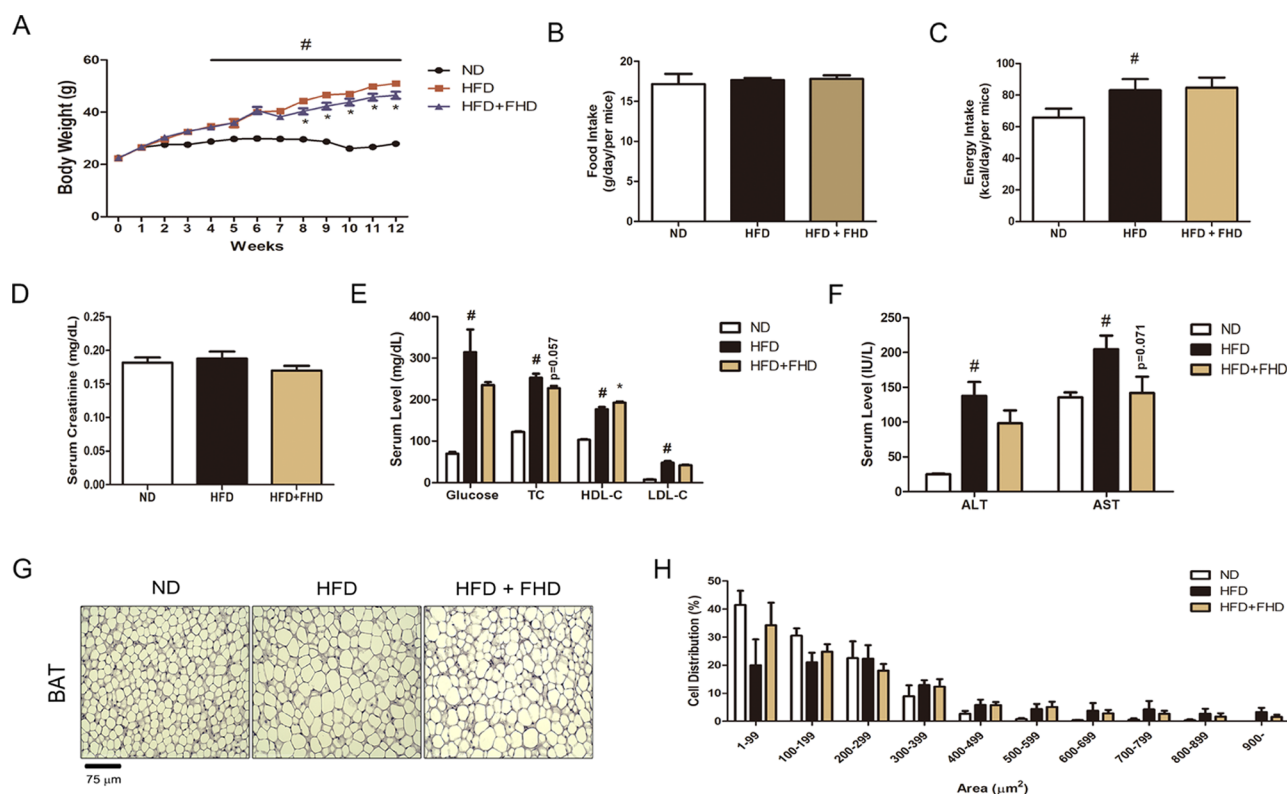


**Figure 1.** Effects of FHD on body weight and lipid accumulation in HFD-induced obese C57BL/6 mice. Mice were administered FHD (5 mg/kg/day) for 7 weeks. (A) Changes in body weight were measured. (B) Food intake was measured. (C) Energy intake was calculated by diet ingredients. Serum levels of (D) creatinine, (E) glucose, TC, HDL-C, LDL-C, (F) ALT, and AST levels were measured. (G) Paraffin-embedded BAT sections from ND, HFD, and HFD with FHD-treated mice were stained with H&E (original magnification, 400 $\times$ ). (H) Lipid droplet diameters were measured, and the percentages of different size lipids were calculated. All values are mean  $\pm$  S.E.M. of data from three separate experiments. <sup>#</sup> $p$  < 0.05 vs ND-fed mice; \* $p$  < 0.05 vs HFD-fed mice. BAT, brown adipose tissue; HFD, high-fat diet; ND, normal diet; FHD, fruits of *H. dulcis* Thunb.

20 nM insulin, which was replenished every 2 days. On day 8, over 95% of the cells were fully differentiated into mature brown adipocytes. FHD (10 and 100  $\mu$ g/mL) was prepared in DM on day 2.

**Cell Cytotoxicity Assay.** Cell viability was measured with a Cell Proliferation MTS kit (Promega Co., Madison, WI) after being treated with FHD (10, 100, 500, and 1000  $\mu$ g/mL) for 48 h, as previously described.<sup>23</sup> Absorbance was measured at 490 nm by a VERSAmix microplate reader (Molecular Devices, San Jose, CA).

**Oil Red O Staining.** Intracellular triglyceride (TG) accumulation was measured using the Oil Red O staining method as previously described.<sup>20</sup> Images were obtained under a regular light microscope (Olympus, Shinjuku, Tokyo, Japan), and absorbance was measured at 500 nm using a VERSAmix microplate reader (Molecular Devices, San Jose, CA).

**RNA Isolation and Quantitative PCR (qPCR).** Total RNA was extracted using a GeneAllR RiboEx total RNA extraction kit (GeneAll Biotechnology, Seoul, Korea). Newly synthesized complementary DNA (cDNA) from FHD-treated brown adipocytes was amplified using specific primers and the Fast SYBR Green PCR master mix (Applied Biosystems, Foster City, CA). mRNA expression was measured with a StepOnePlus qPCR System and StepOne Software v2.1 (Applied Biosystems, Foster City, CA). The primers used in the experiments are shown in Table 1.

**Protein Extraction and Western Blot Analysis.** Western blot analyses were performed as previously described.<sup>22</sup> Briefly, homogenized tissues or harvested cells were lysed in lysis buffer (Cell Signaling Technology, Beverly, MA), and the protein concentration was determined. Protein was resolved by 10–15% sodium dodecyl sulfate-polyacrylamide gel electrophoresis. After transfer, the polyvinylidene difluoride membranes were incubated with the indicated primary antibody at 4  $^{\circ}$ C overnight and then incubated with the

proper horseradish peroxidase (HRP)-conjugated secondary antibody (Jackson Immuno Research, West Grove, PA).

**Mitochondrial Microscopic Analysis.** For mitochondria detection, the cells were incubated with Mito-Tracker Red CMXRos (Molecular Probes, Eugene, OR). After the staining was complete, the solution was replaced with fresh media and fluorescent signals were obtained using an EVOS M7000 system (Thermo Fisher Scientific, Waltham, MA) as previously described.<sup>24</sup>

**DNA Isolation and Mitochondrial DNA (mtDNA) Copy Number Measurement.** Whole-genomic DNA from primary cultured brown adipocytes were isolated using the AccuPrep Genomic DNA extraction kit (Bioneer, Daejeon, Korea) according to the manufacturer's protocol. mtDNA copy number was measured by qPCR using the Mouse mtDNA copy number kit (MCN2) (Detroit R&D, Inc., Detroit, MI).

**Total Intracellular NAD<sup>+</sup> Assay.** The harvested cells were lysed with the reduced nicotinamide adenine dinucleotide (NADH)/NAD extraction buffer and centrifuged. The NAD assay was performed in the collected supernatant using the NAD/NADH assay kit (Abcam, Cambridge, MA) according to the manufacturer's protocol. The measured values were normalized to lysate protein levels. The absorbance was measured at 450 nm in a VERSAmix microplate reader (Molecular Devices, San Jose, CA).

**Oxygen Consumption Analysis.** Oxygen consumption was measured by the Mito-ID extracellular O<sub>2</sub> sensor kit (Enzo Life Science, Lausen, Switzerland). Primary cultured brown adipocytes were differentiated as previously described. When full differentiation of the cells was achieved, the O<sub>2</sub> sensor probe was added into each well. After covering with two drops of Mito-ID HS oil, the plates were read at 380 nm for excitation and 650 nm of emission using a VARIOSKAN LUX spectrophotometer (Thermo Fisher Scientific,

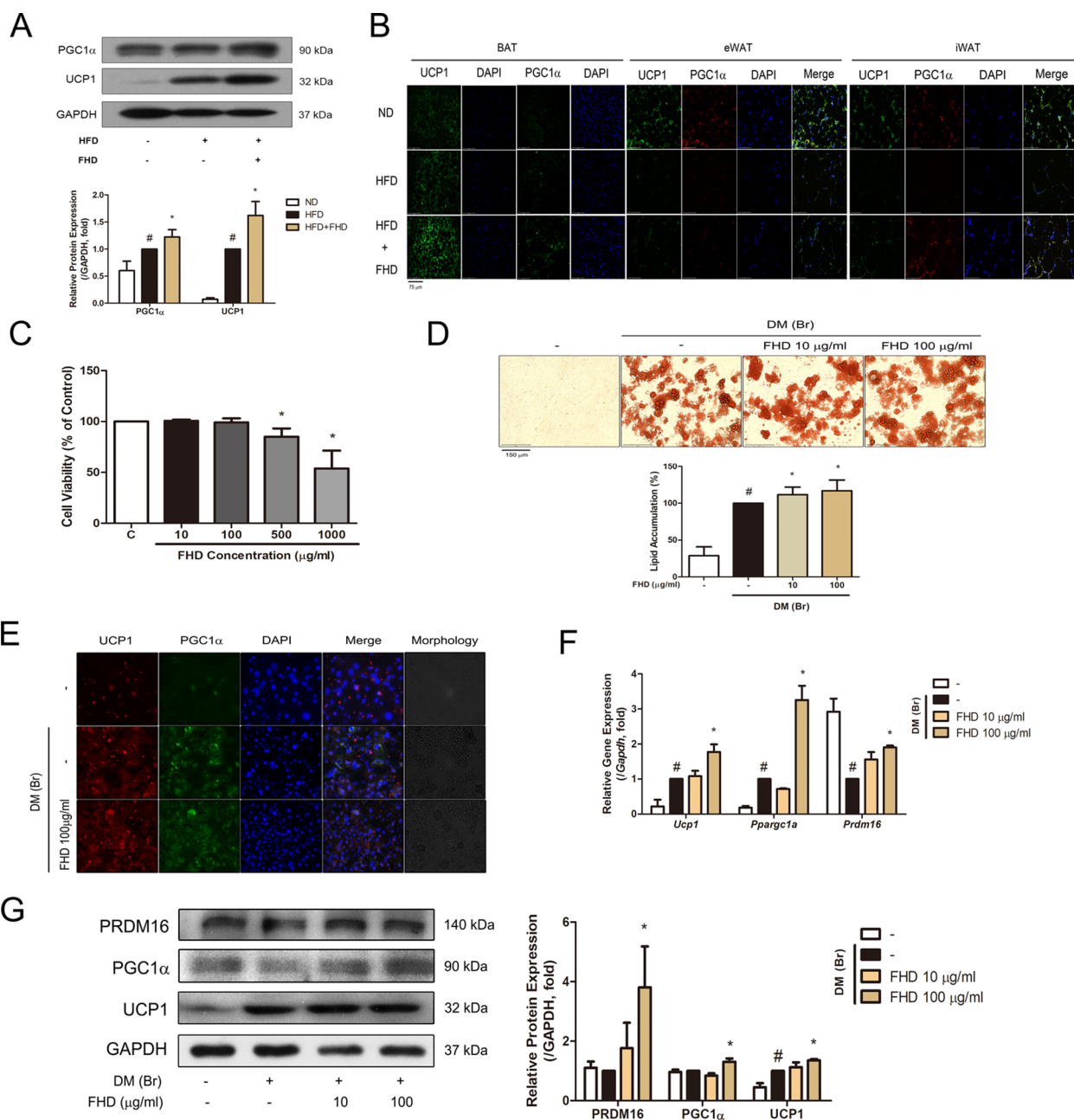


**Figure 2.** Effects of FHD on the regulation expressions of thermogenesis-associated factors in BAT of HFD-induced obese C57BL/6 mice and primary cultured brown adipocytes. (A) Protein levels of UCP1 and PGC1 $\alpha$  were analyzed by Western blot analysis. (B) Paraffin-embedded BAT, eWAT, and iWAT sections from ND, HFD, and HFD with FHD-treated mice were immunostained with antibodies for UCP1 and PGC1 $\alpha$  and counterstained with DAPI for visualization of the cell nucleus (original magnification, 400 $\times$ ). (C) Primary cultured brown adipocytes were incubated with FHD at the indicated concentrations (10, 100, 500, and 1000  $\mu$ g/mL) for 48 h, and cell viability was assessed by the 3-(4,5-dimethylthiazol-2-yl)-5-(3-carboxymethoxyphenyl)-2-(4-sulfophenyl)-2H-tetrazolium (MTS) assay. (D) Primary brown cultured adipocytes were differentiated in the absence or presence of FHD (10 and 100  $\mu$ g/mL). Lipid droplets were measured by Oil Red O staining (original magnification, 200 $\times$ ). (E) Primary cultured brown adipocytes were immunostained with antibodies for UCP1 and PGC1 $\alpha$  and counterstained with DAPI for visualization of the cell nucleus. (F) The mRNA of *Ucp1*, *Ppargc1a*, and *Prdm16* were analyzed by qPCR. (G) Protein levels of UCP1, PGC1 $\alpha$ , and PRDM16 were analyzed by Western blot analysis. Results were expressed relative to GAPDH. All values are the means  $\pm$  S.E.M. of data from three independent experiments. #  $p < 0.05$ , vs ND-fed mice or DM-undifferentiated control cells; \*  $p < 0.05$ , vs HFD-fed mice or DM-differentiated control cells. BAT, brown adipose tissue; HFD, high-fat diet; ND, normal diet; DM, differentiated medium; FHD, fruits of *H. dulcis* Thunb.

Waltham, MA). Normalization was done according to the cell number, which was assessed by 4',6-diamidino-2-phenylindole (DAPI) measurement.

**SIRT1 Gene Silencing by Small Interfering RNA (siRNA).** Predesigned small interfering RNA (siRNA) against SIRT1 and negative control siRNA were purchased from Origene (Rockville,

MD). Transfection into primary cultured brown adipocytes was performed with Lipofectamine RNAiMAX (Thermo Fisher Scientific, Waltham, MA).

**SIRT1 Activity Assay.** SIRT1 activity was measured using an SIRT1 direct fluorescent screening assay kit (Cayman, Ann Arbor, MI), following the manufacturer's protocol. The absorbance was

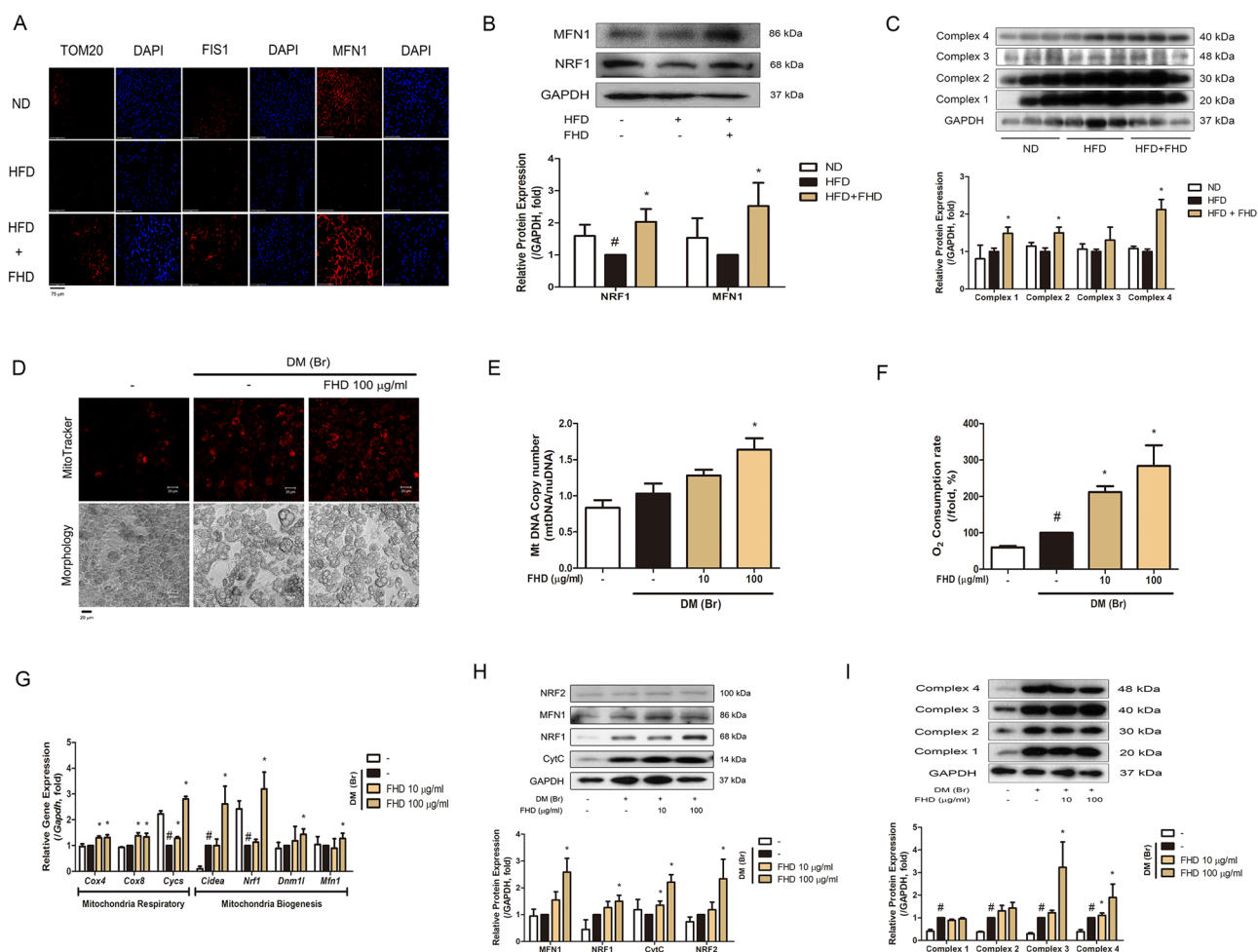


**Figure 3.** Effects of FHD on the regulation of mitochondria-related factors in BAT of HFD-induced obese C57BL/6 mice and primary cultured brown adipocytes. (A) Paraffin-embedded BAT sections from ND, HFD, and HFD with FHD-treated mice were immune-stained with antibodies for TOM20, MFN1, and FIS1 and counterstained with DAPI for visualization of the cell nucleus. (B) Protein levels of NRF1 and MFN1 were analyzed by Western blot analysis in BAT. (C) OXPHOS complex protein levels were analyzed by Western blot analysis in BAT. (D) Mitochondrial abundance in primary cultured brown adipocytes was analyzed by MitoTracker red staining. (E) Mitochondrial DNA copy number in primary cultured brown adipocytes was assessed by qPCR. Mitochondrial DNA was normalized by mouse nuclear DNA. (F) Oxygen consumption in primary cultured brown adipocytes was analyzed. (G) mRNA of *Cox4*, *Cox8*, *Cidea*, *Cysc*, *Nrf1*, *Dnm1l*, and *Mfn1* were analyzed by qPCR in primary cultured brown adipocytes. (H) Protein levels of NRF2, NRF1, MFN1, and CytC were analyzed by Western blot analysis in primary cultured brown adipocytes. (I) OXPHOS complex protein levels were analyzed by Western blot analysis in primary cultured brown adipocytes. Results were expressed relative to GAPDH. All values are mean  $\pm$  S.E.M. of data from three separate experiments. #  $p < 0.05$ , vs ND-fed mice or DM-undifferentiated control cells; \*  $p < 0.05$ , vs HFD-fed mice or DM-differentiated control cells. BAT, brown adipose tissue; HFD, high-fat diet; ND, normal diet; DM, differentiated medium; FHD, fruits of *H. dulcis* Thunb.

measured using a VARIOSKAN LUX spectrophotometer (Thermo Fisher Scientific, Waltham, MA) at an excitation wavelength of 355 nm and an emission wavelength of 460 nm.

**Statistical Analysis.** Data are expressed as mean  $\pm$  standard error mean (S.E.M.). Statistical significance ( $p < 0.05$ ) is determined using a *t*-test or an analysis of variance (ANOVA) followed by a post hoc test of Bonferroni's method unless mentioned otherwise. All statistical analyses were performed using SPSS statistical analysis software version 11.5 (SPSS Inc., Chicago, IL).

## RESULTS

**FHD Decreases Body Weight and Lipid Size of BAT in HFD-Induced Obese C57BL/6 Mice.** First, we investigated whether FHD regulates body weight gain in an obesity mouse model. After inducing obesity by HFD for 4 weeks, the mice were subdivided into two groups ( $n = 6$  per group): the HFD group and the HFD with FHD (5 mg/(kg day)) treatment group. These groups had similar body weights at the beginning

of the study; however, HFD feeding significantly increased the body weight compared to ND. However, in the FHD treatment group, the mice showed significantly reduced body weight of 8.88% than the HFD-fed group (Figure 1A). Food intake was the same for all groups (Figure 1B). When the energy intake was calculated and compared to ND-fed mice, it was increased in both the HFD-fed group and the FHD-fed group but without any significance between the two (Figure 1C). After sacrifice, a plasma parameter analysis was conducted to measure serum TC, LDL-C, HDL-C, glucose, ALT, AST, and creatinine. The serum creatinine level remained unchanged in FHD-fed mice (Figure 1D). The FHD-fed group showed lower numbers in the levels of glucose and TC compared to the HFD-fed mice but without statistical significance (Figure 1E). In addition, FHD raised the level of HDL-C (Figure 1E). The serum levels of ALT and AST were relatively lower in FHD-fed mice ( $p > 0.05$ ) (Figure 1F). From

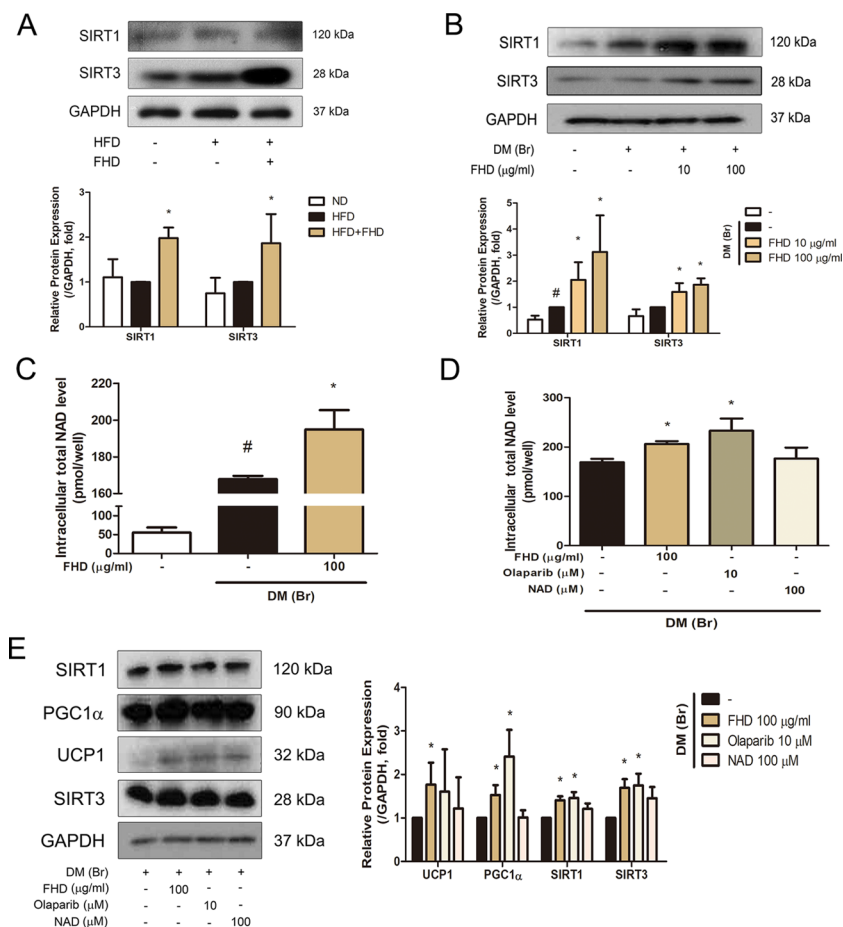


**Figure 4.** Effects of FHD on the activation of the SIRT family in BAT of HFD-induced obese CS7BL/6 mice and primary cultured brown adipocytes. (A) Protein levels of SIRT1 and SIRT3 were analyzed by Western blot analysis in BAT of HFD-induced obese CS7BL/6 mice (B) and primary cultured brown adipocytes. (C, D) Total intracellular NAD<sup>+</sup> in primary cultured brown adipocytes was analyzed. (E) Protein levels of SIRT1, SIRT3, UCP1, and PGC1 $\alpha$  were analyzed by Western blot analysis. Results were expressed relative to GAPDH. All values are mean  $\pm$  S.E.M. of data from three separate experiments. # $p$  < 0.05, vs ND-fed mice or DM-undifferentiated control cells; \* $p$  < 0.05, vs HFD-fed mice or DM-differentiated control cells. BAT, brown adipose tissue; HFD, high-fat diet; ND, normal diet; DM, differentiated medium; FHD, fruits of *H. dulcis* Thunb.

H&E staining of BAT, the size of lipid droplets was decreased by FHD treatment (Figure 1G,H).

**FHD Upregulates Thermogenesis-Related Factors in BAT of HFD-Fed Obese Mice and Primary Cultured Brown Adipocytes.** A major tissue of nonshivering thermogenesis is BAT, in which heat is produced by UCP1.<sup>2</sup> Thus, we investigated whether FHD can induce thermogenic factors in BAT. The protein expressions of UCP1 and PGC1 $\alpha$ , which are specific markers of nonshivering thermogenesis, were significantly increased in BAT of the FHD-fed group compared to obese mice (Figure 2A). IF analyses showed increased expressions of UCP1 and PGC1 $\alpha$  in BAT of FHD-fed mice as seen in Figure 2B. Also, UCP1 and PGC1 $\alpha$  expressions were increased in iWAT of FHD-fed mice in eWAT, showing no alteration in the thermogenic factors (Figure 2B).

To investigate the related mechanisms of the thermogenic effect of FHD, in vitro studies using primary cultured brown adipocytes were carried out. First, to measure the cytotoxicity of FHD in primary cultured brown adipocytes, the cells were treated with FHD (10–1000  $\mu$ g/mL), and the MTS assay was performed. Treatment with 10 and 100  $\mu$ g/mL FHD did not display cytotoxicity in primary cultured brown adipocytes (Figure 2C); thus, these two concentrations were chosen for

further experiments. Next, to determine the effects of FHD on brown adipocyte differentiation, TG accumulation was measured by Oil Red O staining after FHD treatment. Results showed that lipid accumulation was significantly increased by FHD (10 and 100  $\mu$ g/mL) in primary cultured brown adipocytes (Figure 2D). UCP1 and PGC1 $\alpha$  were also increased with the FHD treatment, located in the cytoplasm of primary cultured brown adipocytes, consistent with the in vivo results (Figure 2E). qPCR results showed that thermogenesis-related genes including *Ucp1*, *Ppargc1a*, and *Prdm16* were upregulated in FHD-treated cells (Figure 2F). The protein expressions of PRDM16, PGC1 $\alpha$ , and UCP1 in primary cultured brown adipocytes significantly increased with FHD as well (Figure 2G). These results suggest that FHD can activate thermogenesis-related factors in vivo and in vitro.

**FHD Increases Mitochondria-Related Factors in BAT of HFD-Fed Obese Mice and Primary Cultured Brown Adipocytes.** Thermogenic activation of brown adipocytes is highly dependent on mitochondrial biogenesis.<sup>7</sup> Therefore, we investigated whether FHD can activate mitochondria in BAT of HFD-fed obese mice and primary cultured brown adipocytes. First, mitochondria-related factors by FHD were determined in BAT. As seen in Figure 3A, IF staining of

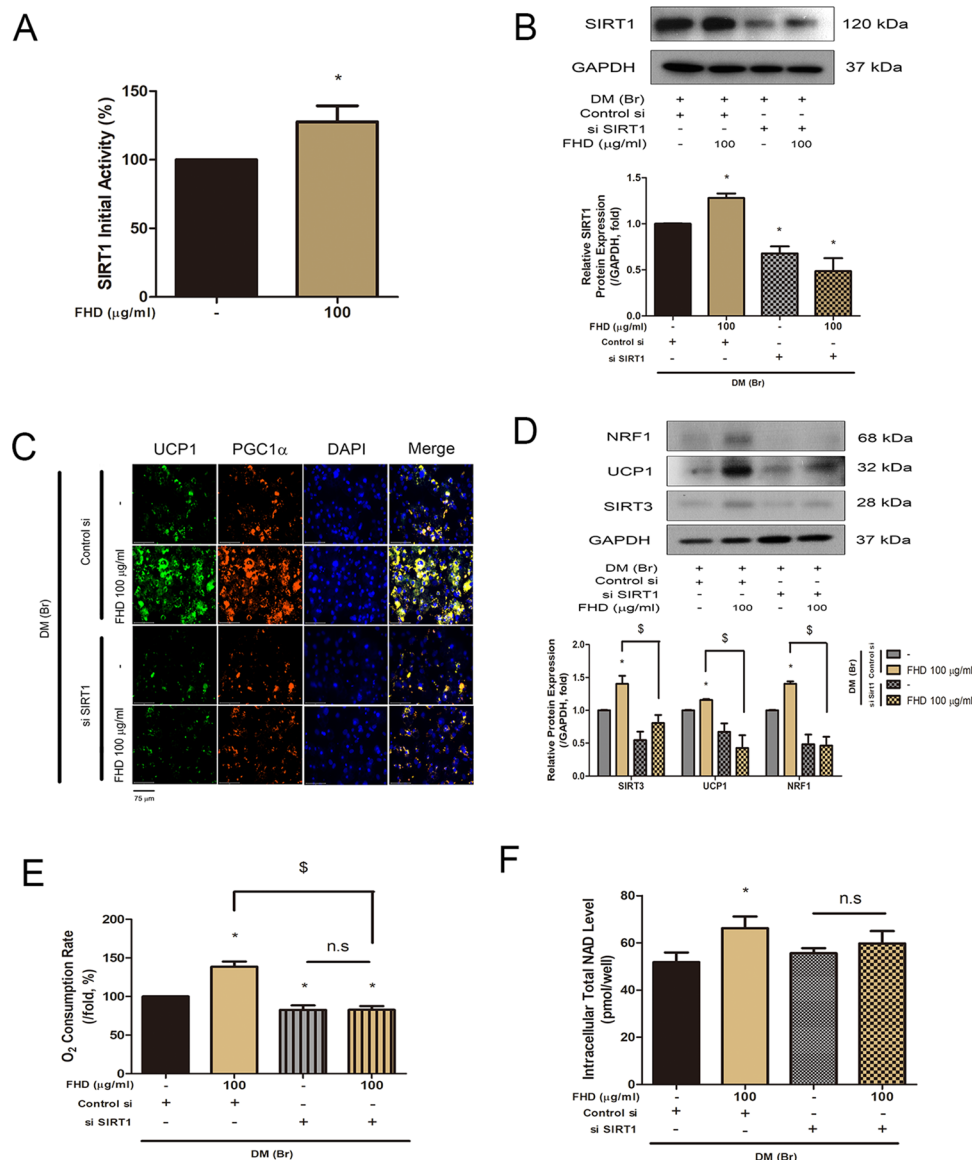


**Figure 5.** Involvement of SIRT1 on the thermogenic activation of FHD in primary cultured brown adipocytes. (A) SIRT1 activity was measured. (B) After treatment with siSIRT1 (10 pM), the protein level of SIRT1 was analyzed by Western blot analysis in primary cultured brown adipocytes. (C) Primary cultured brown adipocytes were immunostained with antibodies for UCP1 and PGC1 $\alpha$  and counterstained with DAPI for visualization of the cell nucleus. (D) Protein levels of SIRT3, UCP1, PGC1 $\alpha$ , and NRF1 were analyzed by Western blot analysis in primary cultured brown adipocytes. (E) Oxygen consumption in primary cultured brown adipocytes was analyzed. (F) Total intracellular NAD<sup>+</sup> in primary cultured brown adipocytes was analyzed. Results were expressed relative to GAPDH. All values are mean  $\pm$  S.E.M. of data from three separate experiments. \* $p$  < 0.05, vs control SI-treated DM-differentiated cells;  $\$$  $p$  < 0.05, vs control SI with FHD-treated DM-differentiated cells. DM, differentiated medium; FHD, fruits of *H. dulcis* Thunb.

mitochondrial biogenesis markers such as FIS1, MFN1, and TOM20 in BAT of HFD-fed obese mice verified the mitochondria proliferative action of FHD. The HFD-fed mice with FHD treatment also showed increased protein levels of MFN1 and NRF1, both of which are involved in mitochondrial activation (Figure 3B). The mitochondrial OXPHOS complex that participates in mitochondrial biogenesis and  $\beta$ -oxidation was also examined. FHD treatment significantly increased the protein levels of complexes 1, 2, and 4 (Figure 3C). These results indicate that FHD can induce mitochondrial biogenesis and activation in BAT.

To confirm the abundance of mitochondria, we stained mitochondria using MitoTracker and measured the mtDNA copy number in primary cultured brown adipocytes. FHD

treatment increased the mitochondrial number and DNA when compared to vehicle treatment (Figure 3D,E). Furthermore, the oxygen consumption significantly increased in FHD-treated primary cultured brown adipocytes (Figure 3F). In addition, mRNA levels of mitochondria-related genes such as *Cox4*, *Cox8*, *Cyts*, *Cidea*, *Nrf1*, *Dnm1l*, and *Mfn1* were significantly increased in a dose-dependent manner with FHD treatment (Figure 3G). In line, the protein levels of NRF2, MFN1, NRF1, and CytC were increased by FHD (Figure 3H). Then, when the expression of the OXPHOS complex in primary cultured brown adipocytes was determined, we observed that the levels of OXPHOS complexes 3 and 4 were significantly increased by FHD (Figure 3I). These results clearly indicate that FHD can activate mitochondria by

increasing mitochondrial biogenesis and the OXPHOS system in primary cultured brown adipocytes.

#### FHD Activates the SIRT Family in BAT of HFD-Fed Obese Mice and Primary Cultured Brown Adipocytes.

We confirmed that FHD induces nonshivering thermogenesis by activating mitochondria and its biogenesis in BAT and primary cultured brown adipocytes. Next, the mechanism of action of FHD on such a fact was investigated. First, we studied whether FHD alters the levels of the SIRT family, which is a well-known regulator of mitochondrial activation.<sup>25</sup> We found that the FHD treatment showed significantly higher levels of SIRT1 and SIRT3 expressions than that of the control group, in both the BAT of HFD-fed mice and primary cultured brown adipocytes (Figure 4A,B). Next, the intracellular NAD<sup>+</sup> expression level, one of the upstream regulators of the SIRT family, was confirmed in FHD-treated primary cultured brown adipocytes. FHD clearly increased the intracellular NAD<sup>+</sup> level (Figure 4C). To confirm the capability of FHD as a NAD regulator, FHD, NAD<sup>+</sup>, and the NAD activator Olaparib were treated in primary cultured brown adipocytes, sequentially. The level of intracellular NAD<sup>+</sup> was increased by both FHD and Olaparib treatment; however, the NAD<sup>+</sup>-treated group did not show such a change (Figure 4D). Then, the SIRT1, SIRT3, PGC1 $\alpha$ , and UCP1 proteins were investigated after these treatments. FHD and Olaparib treatment increased levels of SIRT1, SIRT3, PGC1 $\alpha$ , and UCP1; however, no statistical difference was observed in the UCP1 expression of Olaparib-treated cells (Figure 4E). These results suggest that FHD can act as an inducer of intracellular NAD<sup>+</sup> levels.

#### Thermogenic Activation of FHD Is Dependent on SIRT1 in Primary Cultured Brown Adipocytes.

From the above results, we deduced that FHD induces SIRT, a NAD-dependent deacetylase protein,<sup>25</sup> and intracellular NAD<sup>+</sup> levels in primary cultured brown adipocytes. To confirm these results, we first measured the effect of FHD on SIRT1 activity. FHD treatment increased the activity of SIRT1 up to 140% (Figure 5A). Then, primary cultured brown adipocytes were pretreated with SIRT1 siRNA to create an SIRT1-inhibited condition to verify the action mechanism of FHD. As shown in Figure 5B, SIRT1 protein levels were reduced by SIRT1 siRNA treatment. When SIRT1 was silenced by SIRT1 siRNA, IF showed that FHD did not increase the expressions of PGC1 $\alpha$  and UCP1, which were significantly induced in the control siRNA with FHD-treated cells (Figure 5C). Also, FHD failed to increase the protein expressions of PGC1 $\alpha$ , NRF1, UCP1, and SIRT3 (Figure 5D). Furthermore, when SIRT1 was silenced, FHD could not increase oxygen consumption and intracellular NAD<sup>+</sup> levels (Figure 5E,F). This suggests that the mitochondrial activation and thermogenic action of FHD are dependent on the SIRT1 pathway.

## DISCUSSION

There are two different subtypes of adipose tissues in humans: WAT and BAT. WAT and BAT have opposing functions in terms of energy homeostasis.<sup>26</sup> In the past, the physiological relevance of BAT was believed to be limited since the tissue is present only in early childhood and disappears with age. However, recent studies have shown that BAT does exist in the upper-chest and neck regions of adult humans.<sup>1,2</sup> Moreover, functionwise, these studies reported that BAT acts as an effector for nonshivering thermogenesis and lipid metabolism, with an increase in the density of BAT detected by PET scan. Activating brown adipocyte differentiation increases energy

expenditure by mitochondria and in turn reduces body weight, whereas decreased brown adipocyte differentiation is related to obesity and insulin resistance.<sup>27,28</sup> Given these findings, the importance of BAT has recently gained massive interest, especially as a promising therapeutic target to treat obesity.

Recent studies have provided evidence on the beneficial effect of FHD in hepatic diseases. For example, one study showed that FHD has a hepatoprotective effect by homeostatic regulation of the inflammatory reaction.<sup>29</sup> Another study suggested that FHD reduces lipogenesis and cholesterol synthesis in fatty liver diseases.<sup>30</sup> Since excessive obesity is associated with hepatic disease, researchers argued that FHD has an obesity treatment effect. Also, we previously reported the inhibitory effect of FHD on adipogenesis by the AMPK pathway in 3T3-L1 cells.<sup>20</sup> However, the study was limited to an antiadipogenic effect on white-differentiated adipocytes, and the antiobese effect through the thermogenic activation is unknown. In addition, FHD were found to have no effect on the phosphorylation of AMPK $\alpha$  in primary cultured brown adipocytes and BAT in the present study (Figure S1 of the Supporting Information). In our previous study, the phytochemical profile of FHD using high-performance liquid chromatography (HPLC) and gas chromatography-mass spectrometry (GC-MS) analysis identified 2,3-dihydro-3,5-dihydroxy-6-methyl-4(*H*)-pyran-4-one, 5-hydroxymethyl-2-furancarboxaldehyde, and quercetin.<sup>20</sup> 2,3-Dihydro-3,5-dihydroxy-6-methyl-4(*H*)-pyran-4-one was shown to increase the BAT sympathetic nerve activity and the body temperature above the interscapular brown adipose tissue in rats.<sup>31</sup> Quercetin is also well known to display a thermogenesis-mediated antiobesity effect.<sup>32,33</sup> In a study by Kaşıkçı et al.,<sup>34</sup> quercetin showed oral bioavailability of about 24%, which was slightly lower compared to 52% of isoquercetin, another component of FHD. In another study, quercetin showed 44.8% bioavailability.<sup>35</sup> These reports on the absorbance of constituents of FHD suggest its possible use as an orally administered agent.

Obesity is mainly due to the accumulation of lipids; changes in the morphology of adipose tissue can be used as a measure of obesity.<sup>36</sup> In the present study, FHD reduced body weight gain in HFD-fed mice. But energy intake and food intake in the FHD group were the same as in the HFD-fed group. These results suggest that FHD reduces weight gain regardless of diet. FHD increased serum HDL-C levels and decreased the serum TC level. FHD also decreased the distribution of lipid droplet size in BAT of HFD-fed mice. From these results, we believed that FHD had an antiobese activity in HFD-induced obese mice. We then investigated whether FHD shows an antiobesity effect through thermogenic activity.

Brown adipocytes have an abundance of mitochondria, especially UCP1, which is in the mitochondrial inner membrane, and is very important in the thermogenic action.<sup>37</sup> The thermogenic action of BAT consumes lipids without ATP production and strongly depends on the activity of UCP1.<sup>38</sup> PGC1 $\alpha$  is also involved in thermogenic action with UCP1.<sup>39</sup> FHD increased UCP1 and PGC1 $\alpha$  levels in BAT as well as iWAT of HFD-fed mice. However, when we measured the rectal temperature, there was no change in body temperature by FHD treatment (Figure S2 of the Supporting Information). The *in vivo* study was further supported by *in vitro* experiments. FHD up to 100  $\mu$ g/mL did not cause significant cytotoxic effects while inducing brown adipocyte differentiation and upregulating thermogenic factors such as

UCP1 and PGC1 $\alpha$  in primary cultured brown adipocytes. Furthermore, PRDM16, a transcription coregulator in the development of brown adipocytes, as well as UCP1 and PGC1 $\alpha$  also increased based on the dose of FHD in primary cultured brown adipocytes.

In addition, FHD increased the levels of mitochondria biogenesis-related proteins such as MFN1, NRF1, TOM20, and FIS1 in BAT of HFD-fed mice. FHD also induced gene levels of such factors, including *Cox4*, *Cox8*, *Nrf1*, *Cidea*, *Cyts*, *Dnm1l*, and *Mfn1* in primary cultured brown adipocytes. MFN1, DLP1, and FIS1 are associated with mitochondria fusion and fission. An ongoing mitochondrial fusion/fission cycle drives the functional, genetic complementation, and the proper distribution of mitochondria.<sup>40</sup> NRF is a transcription factor that stimulates nuclear genes such as CytC, a critical factor in the proper functioning of mitochondria.<sup>41</sup> TOM20, a protein complex located at the outer membrane of mitochondria,<sup>42</sup> allows movement of proteins into the intermembrane of the mitochondria.<sup>43</sup> Increased expression of TOM20 is a way to determine the number of mitochondria. Mitochondrial content is also expressed as a copy number, which is maintained in a relatively safe range to meet the energy needs of cells to preserve normal physiological function.<sup>44</sup> As shown in TOM20/MitoTracker IF staining and qPCR, FHD increased mitochondrial mass in both mitochondrial number and DNA in primary cultured brown adipocytes. These results indicate that FHD has a thermogenic action and it induces thermogenesis through activating mitochondrial biogenesis in brown adipocytes.

Our results showed that activation of the OXPHOS complex as well as oxygen consumption was caused by FHD in BAT and primary cultured brown adipocytes. The OXPHOS complex function is the metabolic pathway inside the mitochondria of cells.<sup>45,46</sup> During OXPHOS activation, electrons are transferred from electron donors to acceptors such as oxygen and thereby release energy, which is used to form ATP.<sup>47</sup> Since ATP production through OXPHOS in mitochondria is essential for energy expenditure, the increase of the OXPHOS system by FHD can be a potential evidence in the antiobesity effect of FHD. The OXPHOS complex not only plays a role in energy expenditure but also contributes to the formation of electron gradients for the thermogenic activation by UCP1. Therefore, from the above-mentioned results, we suggest that FHD activates mitochondrial biogenesis and thermogenesis as well energy consumption via the OXPHOS system and resulted in the regulation of body weight of obese mice.

Subsequently, we found that FHD activates mitochondrial biogenesis and thermogenesis in BAT and brown adipocytes. Then, we determined which signal pathway FHD regulates and results in mitochondrial activation. The SIRT family is one of the notably increased thermogenic and mitochondrial factors.<sup>48,49</sup> From our experiments, SIRT1 and SIRT3 were significantly increased by FHD in BAT of HFD-fed mice and primary cultured brown adipocytes. The SIRT family influences a wide range of cellular processes like aging, transcription, apoptosis, and inflammation.<sup>50,51</sup> Also, the SIRT family is associated with the control and increase of mitochondrial biogenesis in brown adipocytes.<sup>52</sup> Therefore, we suggest that FHD activates mitochondrial biogenesis by increasing SIRT1. The NAD<sup>+</sup> levels are metabolic coenzymes and also substrates involved in cellular energy metabolism and energy production results in deacetylation/activation of

PGC1 $\alpha$ . In addition, increased NAD<sup>+</sup> levels result in the activation of the SIRT family.<sup>53,54</sup> The intracellular NAD<sup>+</sup> level is increased by FHD and Olaparib, a NAD inducer, which has been shown in a previous study to induce browning of human primary white adipocytes.<sup>55</sup> However, NAD<sup>+</sup> treatment did not induce any changes in brown adipocytes. Also, FHD and Olaparib significantly increased the expressions of SIRT1, SIRT3, PGC1 $\alpha$ , and UCP1 proteins. From these facts, we can hypothesize that FHD increases intracellular NAD<sup>+</sup> and induces the SIRT family expression, thereby activating mitochondrial biogenesis and thermogenesis. Furthermore, we investigated whether the mitochondrial activation and thermogenic activity by FHD are abolished in limited SIRT activities. From our results, we demonstrated that the SIRT1 gene silencing resulted in the reduction of mitochondria and its thermogenic activities. SIRT3 is also an important member of the sirtuin family, which is responsible for the mitochondrial action during nonshivering thermogenesis of BAT.<sup>56</sup> Our results demonstrate that FHD treatment increased expressions of SIRT1 and SIRT3 both; however, fold change was comparably higher in SIRT1. Therefore, we rather concentrated on the role of SIRT1 in the action mechanism of FHD. Yet, close investigation should be carried out to elucidate the exact role of SIRT3 in the action mechanism of FHD. Based on our results, we conclude that FHD has the action for mitochondrial biogenesis and activation and these actions are dependent on the SIRT1 pathway.

## ■ ASSOCIATED CONTENT

### Supporting Information

The Supporting Information is available free of charge at <https://pubs.acs.org/doi/10.1021/acs.jafc.0c01117>.

Composition of experimental diets (Table S1); effect of FHD on activation of AMPK $\alpha$  in BAT of HFD-induced obese C57BL/6 mice and primary cultured brown adipocytes (Figure S1); effect of FHD on rectal temperature in HFD-induced obese C57BL/6 mice (Figure S2) (PDF)

## ■ AUTHOR INFORMATION

### Corresponding Author

Jae-Young Um – Department of Pharmacology, College of Korean Medicine and Department of Comorbidity Research, KyungHee Institute of Convergence Korean Medicine, Kyung Hee University, Seoul 02447, Republic of Korea; [orcid.org/0000-0002-0568-9738](https://orcid.org/0000-0002-0568-9738); Email: [jyum@khu.ac.kr](mailto:jyum@khu.ac.kr)

### Authors

Gahe Song – Department of Science in Korean Medicine, Graduate School, Kyung Hee University, Seoul 02447, Republic of Korea

Hye-Lin Kim – Department of Pharmacology, College of Korean Medicine and Department of Comorbidity Research, KyungHee Institute of Convergence Korean Medicine, Kyung Hee University, Seoul 02447, Republic of Korea

Yunu Jung – Department of Pharmacology, College of Korean Medicine and Department of Comorbidity Research, KyungHee Institute of Convergence Korean Medicine, Kyung Hee University, Seoul 02447, Republic of Korea

Jinbong Park – Department of Pharmacology, College of Korean Medicine and Department of Comorbidity Research, KyungHee

Institute of Convergence Korean Medicine, Kyung Hee University, Seoul 02447, Republic of Korea

**Jun Hee Lee** – Department of Comorbidity Research, KyungHee Institute of Convergence Korean Medicine and Department of Sasang Constitutional Medicine, College of Korean Medicine, Kyung Hee University, Seoul 02447, Republic of Korea

**Kwang Seok Ahn** – Department of Comorbidity Research, KyungHee Institute of Convergence Korean Medicine, Kyung Hee University, Seoul 02447, Republic of Korea

**Hyun Jeong Kwak** – Department of Life Science, College of Natural Sciences, Kyonggi University, Suwon 16227, Republic of Korea

Complete contact information is available at:  
<https://pubs.acs.org/10.1021/acs.jafc.0c01117>

### Author Contributions

This study was supported by the National Research Foundation of Korea (NRF) grant funded by the Korea government (NRF-2015R1A4A1042399, 2017M3A9E4065333, 2018R1A2A3075684, and 2019R1I1A1A01062419).

### Notes

The authors declare no competing financial interest.

### REFERENCES

(1) Cypess, A. M.; Lehman, S.; Williams, G.; Tal, I.; et al. Identification and importance of brown adipose tissue in adult humans. *N. Engl. J. Med.* **2009**, *360*, 1509–1517.

(2) van Marken Lichtenbelt, W. D.; Vanhommel, J. W.; Smulders, N. M.; Drossaerts, J. M. A. F. L.; et al. Cold-activated brown adipose tissue in healthy men. *N. Engl. J. Med.* **2009**, *360*, 1500–1508.

(3) Orava, J.; Nuutila, P.; Lidell, M. E.; Oikonen, V.; et al. Different metabolic responses of human brown adipose tissue to activation by cold and insulin. *Cell Metab.* **2011**, *14*, 272–279.

(4) Cypess, A. M.; Weiner, L. S.; Roberts-Toler, C.; Franquet Elia, E.; et al. Activation of human brown adipose tissue by a  $\beta$ 3-adrenergic receptor agonist. *Cell Metab.* **2015**, *21*, 33–38.

(5) Camont, L.; Chapman, M. J.; Kontush, A. Biological activities of HDL subpopulations and their relevance to cardiovascular disease. *Trends Mol. Med.* **2011**, *17*, 594–603.

(6) Goldberg, I. J. Lipoprotein lipase and lipolysis: central roles in lipoprotein metabolism and atherogenesis. *J. Lipid Res.* **1996**, *37*, 693–707.

(7) Klaus, S. Functional differentiation of white and brown adipocytes. *BioEssays* **1997**, *19*, 215–223.

(8) Petrovic, N.; Walden, T. B.; Shabalina, I. G.; Timmons, J. A.; et al. Chronic peroxisome proliferator-activated receptor gamma (PPAR $\gamma$ ) activation of epididymally derived white adipocyte cultures reveals a population of thermogenically competent, UCP1-containing adipocytes molecularly distinct from classic brown adipocytes. *J. Biol. Chem.* **2010**, *285*, 7153–7164.

(9) Mozo, J.; Emre, Y.; Bouillaud, F.; Ricquier, D.; Criscuolo, F. Thermoregulation: what role for UCPs in mammals and birds? *Biosci. Rep.* **2005**, *25*, 227–249.

(10) Chechi, K.; Nedergaard, J.; Richard, D. Brown adipose tissue as an anti-obesity tissue in humans. *Obes. Rev.* **2014**, *15*, 92–106.

(11) Porter, C. Quantification of UCP1 function in human brown adipose tissue. *Adipocyte* **2017**, *6*, 167–174.

(12) Logan, D. C. The mitochondrial compartment. *J. Exp. Bot.* **2006**, *57*, 1225–1243.

(13) Cantó, C.; Menzies, K. J.; Auwerx, J. NAD(+) Metabolism and the Control of Energy Homeostasis: A Balancing Act between Mitochondria and the Nucleus. *Cell Metab.* **2015**, *22*, 31–53.

(14) Bai, P.; Canto, C.; Brunyanszki, A.; Huber, A.; et al. PARP-2 regulates SIRT1 expression and whole-body energy expenditure. *Cell Metab.* **2011**, *13*, 450–460.

(15) Houtkooper, R. H.; Pirinen, E.; Auwerx, J. Sirtuins as regulators of metabolism and healthspan. *Nat. Rev. Mol. Cell Biol.* **2012**, *13*, 225–238.

(16) Schug, T. T.; Li, X. Sirtuin 1 in lipid metabolism and obesity. *Ann. Med.* **2011**, *43*, 198–211.

(17) Haigis, M. C.; Sinclair, D. A. Mammalian sirtuins: biological insights and disease relevance. *Annu. Rev. Pathol. Mech. Dis.* **2010**, *5*, 253–295.

(18) Park, J. S.; Kim, I. S.; Shaheed Ur, R.; Na, C. S.; Yoo, H. H. HPLC Determination of Bioactive Flavonoids in *Hovenia dulcis* Fruit Extracts. *J. Chromatogr. Sci.* **2016**, *54*, 130–135.

(19) Ji, Y.; Chen, S.; Zhang, K.; Wang, W. Effects of *Hovenia dulcis* Thunb on blood sugar and hepatic glycogen in diabetic mice. *Zhongyaocai* **2002**, *25*, 190–191.

(20) Kim, H. L.; Sim, J. E.; Choi, H. M.; Choi, I. Y.; et al. The AMPK pathway mediates an anti-adipogenic effect of fruits of *Hovenia dulcis* Thunb. *Food Funct.* **2014**, *5*, 2961–2968.

(21) Lee, Y. A.; Chae, H. J.; Moon, H. Y. Effect of *Hovenia dulcis* Thunb. var. *koreana* Nakai fruit extract on glucose, lipid metabolism and antioxidant activity in streptozotocin-induced diabetic rats. *J. Exp. Biomed. Sci.* **2005**, *11*, 533–538.

(22) Jung, Y.; Park, J.; Kim, H. L.; Sim, J. E.; et al. Vanillic acid attenuates obesity via activation of the AMPK pathway and thermogenic factors in vivo and in vitro. *FASEB J.* **2018**, *32*, 1388–1402.

(23) Klein, J.; Fasshauer, M.; Ito, M.; Lowell, B. B.; et al. beta(3)-adrenergic stimulation differentially inhibits insulin signaling and decreases insulin-induced glucose uptake in brown adipocytes. *J. Biol. Chem.* **1999**, *274*, 34795–34802.

(24) Jeong, M. Y.; Park, J.; Youn, D. H.; Jung, Y.; et al. Albiflorin ameliorates obesity by inducing thermogenic genes via AMPK and PI3K/AKT in vivo and in vitro. *Metabolism* **2017**, *73*, 85–99.

(25) Kalous, K. S.; Wynia-Smith, S. L.; Olp, M. D.; Smith, B. C. Mechanism of Sirt1 NAD<sup>+</sup>-dependent Protein Deacetylase Inhibition by Cysteine S-Nitrosation. *J. Biol. Chem.* **2016**, *291*, 25398–25410.

(26) Rosen, E. D.; Spiegelman, B. M. Adipocytes as regulators of energy balance and glucose homeostasis. *Nature* **2006**, *444*, 847–853.

(27) Tseng, Y. H.; Kokkotou, E.; Schulz, T. J.; Huang, T. L.; et al. New role of bone morphogenetic protein 7 in brown adipogenesis and energy expenditure. *Nature* **2008**, *454*, 1000–1004.

(28) Yang, X.; Enerback, S.; Smith, U. Reduced expression of FOXC2 and brown adipogenic genes in human subjects with insulin resistance. *Obes. Res.* **2003**, *11*, 1182–1191.

(29) Kim, H.; Kim, Y. J.; Jeong, H. Y.; Kim, J. Y.; et al. A standardized extract of the fruit of *Hovenia dulcis* alleviated alcohol-induced hangover in healthy subjects with heterozygous ALDH2: A randomized, controlled, crossover trial. *J. Ethnopharmacol.* **2017**, *209*, 167–174.

(30) Kim, B.; Woo, M. J.; Park, C. S.; Lee, S. H.; et al. *Hovenia dulcis* Extract Reduces Lipid Accumulation in Oleic Acid-Induced Steatosis of Hep G2 Cells via Activation of AMPK and PPARalpha/CPT-1 Pathway and in Acute Hyperlipidemia Mouse Model. *Phytother. Res.* **2017**, *31*, 132–139.

(31) Beppu, Y.; Komura, H.; Izumo, T.; Horii, Y.; et al. Identification of 2,3-Dihydro-3,5-dihydroxy-6-methyl-4H-pyran-4-one Isolated from *Lactobacillus pentosus* Strain S-PT84 Culture Supernatants as a Compound That Stimulates Autonomic Nerve Activities in Rats. *J. Agric. Food Chem.* **2012**, *60*, 11044–11049.

(32) Choi, H.; Kim, C.-S.; Yu, R. Quercetin Upregulates Uncoupling Protein 1 in White/Brown Adipose Tissues through Sympathetic Stimulation. *J. Obes. Metab. Syndr.* **2018**, *27*, 102–109.

(33) Zhao, Y.; Chen, B.; Shen, J.; Wan, L.; et al. The Beneficial Effects of Quercetin, Curcumin, and Resveratrol in Obesity. *Oxid. Med. Cell. Longevity* **2017**, *2017*, No. 1459497.

(34) Kaşıkçı, M. B.; Bağdatlıoğlu, N. Bioavailability of Quercetin. *Curr. Res. Nutr. Food Sci.* **2016**, *4*, 146–151.

(35) Walle, T.; Walle, U. K.; Halushka, P. V. Carbon dioxide is the major metabolite of quercetin in humans. *J. Nutr.* **2001**, *131*, 2648–2652.

- (36) Berry, R.; Church, C. D.; Gericke, M. T.; Jeffery, E.; et al. Imaging of adipose tissue. *Methods Enzymol.* **2014**, *537*, 47–73.
- (37) Fenzl, A.; Kiefer, F. W. Brown adipose tissue and thermogenesis. *Horm. Mol. Biol. Clin. Invest.* **2014**, *19*, 25–37.
- (38) Brondani, L. d. A.; Assmann, T. S.; Duarte, G. C.; Gross, J. L.; et al. The role of the uncoupling protein 1 (UCP1) on the development of obesity and type 2 diabetes mellitus. *Arq. Bras. Endocrinol. Metabol.* **2012**, *56*, 215–225.
- (39) Ouellet, V.; Labbe, S. M.; Blondin, D. P.; Phoenix, S.; et al. Brown adipose tissue oxidative metabolism contributes to energy expenditure during acute cold exposure in humans. *J. Clin. Invest.* **2012**, *122*, 545–552.
- (40) Seo, A. Y.; Joseph, A. M.; Dutta, D.; Hwang, J. C.; et al. New insights into the role of mitochondria in aging: mitochondrial dynamics and more. *J. Cell Sci.* **2010**, *123*, 2533–2542.
- (41) Scarpulla, R. C. Transcriptional activators and coactivators in the nuclear control of mitochondrial function in mammalian cells. *Gene* **2002**, *286*, 81–89.
- (42) Saitoh, T.; Igura, M.; Obita, T.; Ose, T.; et al. Tom20 recognizes mitochondrial presequences through dynamic equilibrium among multiple bound states. *EMBO J.* **2007**, *26*, 4777–4787.
- (43) Tokatlidis, K.; Vial, S.; Luciano, P.; Vergnolle, M.; Clemence, S. Membrane protein import in yeast mitochondria. *Biochem. Soc. Trans.* **2000**, *28*, 495–499.
- (44) Clay Montier, L. L.; Deng, J. J.; Bai, Y. Number matters: control of mammalian mitochondrial DNA copy number. *J. Genet. Genomics* **2009**, *36*, 125–131.
- (45) Mitchell, P.; Moyle, J. Chemiosmotic Hypothesis of Oxidative Phosphorylation. *Nature* **1967**, *213*, 137–139.
- (46) Formosa, L. E.; Ryan, M. T. Mitochondrial OXPHOS complex assembly lines. *Nat. Cell Biol.* **2018**, *20*, 511–513.
- (47) Cogliati, S.; Enriquez, J. A.; Scorrano, L. Mitochondrial Cristae: Where Beauty Meets Functionality. *Trends Biochem. Sci.* **2016**, *41*, 261–273.
- (48) Baskaran, P.; Krishnan, V.; Fettel, K.; Gao, P.; et al. TRPV1 activation counters diet-induced obesity through sirtuin-1 activation and PRDM-16 deacetylation in brown adipose tissue. *Int. J. Obes.* **2017**, *41*, 739–749.
- (49) Bagul, P. K.; Katare, P. B.; Bugga, P.; Dinda, A. K.; Banerjee, S. K. SIRT-3 Modulation by Resveratrol Improves Mitochondrial Oxidative Phosphorylation in Diabetic Heart through Deacetylation of TFAM. *Cells* **2018**, *7*, No. 235.
- (50) Preyat, N.; Leo, O. Sirtuin deacylases: a molecular link between metabolism and immunity. *J. Leukocyte Biol.* **2013**, *93*, 669–680.
- (51) Satoh, A.; Brace, C. S.; Ben-Josef, G.; West, T.; et al. SIRT1 promotes the central adaptive response to diet restriction through activation of the dorsomedial and lateral nuclei of the hypothalamus. *J. Neurosci.* **2010**, *30*, 10220–10232.
- (52) Shi, T.; Wang, F.; Stieren, E.; Tong, Q. SIRT3, a mitochondrial sirtuin deacetylase, regulates mitochondrial function and thermogenesis in brown adipocytes. *J. Biol. Chem.* **2005**, *280*, 13560–13567.
- (53) Hwang, J. H.; Kim, D. W.; Jo, E. J.; Kim, Y. K.; et al. Pharmacological stimulation of NADH oxidation ameliorates obesity and related phenotypes in mice. *Diabetes* **2009**, *58*, 965–974.
- (54) Li, W.; Sauve, A. A. NAD(+) content and its role in mitochondria. *Methods Mol. Biol.* **2015**, *1241*, 39–48.
- (55) Nagy, L.; Rauch, B.; Balla, N.; Ujlaki, G.; et al. Olaparib induces browning of in vitro cultures of human primary white adipocytes. *Biochem. Pharmacol.* **2019**, *167*, 76–85.
- (56) Sebaa, R.; Johnson, J.; Pileggi, C.; Norgren, M.; et al. SIRT3 Controls Brown Fat Thermogenesis by Deacetylation Regulation of Pathways Upstream of UCP1. *Mol. Metab.* **2019**, *25*, 35–49.